Effect of Binders on the Processing of α-Alumina in Tunnel Kiln

Abhrajit Chatterjee[1], Meerambika Behera[2], Vinod Kumar Verma[3], Kali Sanjay[4], Bijoy Kumar Satpathy[5] and Suraj Kumar Tripathy[6]

1. PhD Student
2. PhD Student
6. Associate Professor

School of Chemical Technology, Kalinga Institute of Industrial Technology, Bhubaneswar, India

3. Manager (R & D), NALCO Alumina Refinery, Damanjodi, India
4. Chief Scientist, CSIR-Institute of Minerals & Materials Technology, Bhubaneswar, India
5. Visiting Scientist, IIT, Bhubaneswar, India

Corresponding author: suraj.tripathy@kiitbiotech.ac.in

Abstract

In today's scenario, most extensively employed binder systems for monolithic refractories are high alumina cements and chemical binders. The ability to choose and apply the best suited binder is critical to the monolithic product's performance. The effects of several types of binders on α-alumina were investigated in this study using a simple technique. It was developed in a two-step method without the involvement of saggars. For greater α-alumina purity, three types of binders were chosen, with PVA (Polyvinyl Alcohol) proving to be the most effective. Effect of binders and increase in temperature are some of the crucial parameters in terms of the purity of alumina. The XRD (X-Ray diffraction) technique was utilised to distinguish between α-alumina and γ-alumina and revealed a structural phase change from gamma-Al_2O_3 to alpha-Al_2O_3 in nano-porous structure. Electron microscopy images indicated the formation of near spherical shape with a diameter roughly to be 25 nm. Further, from the surface morphological studies it was observed that the synthesized α-alumina was at the higher side, although the porosity decreased with temperature. Our research revealed that the synthesized α-alumina has a high purity of 99.9 %, implying that it has the potential for future industrial uses, especially while its production using a tunnel kiln in an economical manner.

Keywords: Aluminium oxide, Binder, Nanomaterial, Phase transition, Synthesis.

1. Introduction

Alumina (Al_2O_3) is a raw material used in the production of many different types of ceramic materials, catalyst supports and refractories. Most commercial alumina is produced according to the "Bayer Process", a well-known process for the production of alumina from bauxite [1]. Alumina has high strength and excellent heat resistance, and they are used in the form of moulded articles [2]. In particular, these products are obtained by moulding and/or mixing alumina together with various binder components and different matrixes having small bulk density and so they are lightweight [3]. In addition, they have a large insulating effect, and therefore they are suitable for high-temperature insulating materials. Having said that, alumina and its applications are effectively applied in various industries for its supremacy in physical and chemical properties which is high heat resistance, excellent electrical isolation, abrasion resistance and high corrosion resistance [4]. In recent years, the demand of high purity alumina is expanding in fields which are expected to show a high growth rate i.e., display materials, energy, automobiles, semiconductors and computers [5,6,7]. The term "high-purity" refers to alumina that is 99.6 % -99.9 % pure and composed of uniformly sized fine particles. When the purity is lower than this level, chemical stability is poor, and the objective of the present invention cannot be achieved. In this connection, alumina blocks prepared with absolute zero dilution with any other external products other than

a binding agent [8,9]. The Bayer processing of bauxite to produce smelter grade alumina involves digestion of the bauxite ore at temperatures in the range of 135-250 °C. The digestion produces a saturated sodium aluminate liquor from which ATH (Aluminium Tri-hydroxide) is crystallized (as gibbsite) by cooling in the presence of large quantities of seeds [10, 11].

In this context, a poor bauxite as defined by commercial practice [12] would have a Total Available Alumina/ reactive silica (TAA/reactive SiO_2) ratio of alumina products are not for smelter use [13]. Alternative processes (non-Bayer) have been developed in efforts to recover alumina from bauxite in an attempt to reduce the cost and energy required for the production of specialty alumina (low soda, fine and high purity alumina). Other processing techniques have been developed in order to produce these more valuable specialty alumina or sodium aluminate etc, [14,15]. New research has also been conducted to develop alternative processes to recover alumina from "hard to treat" bauxites, including those containing high soluble silica or diaspore, aluminogoethite ores or calcium aluminate slags, which pose technical difficulties during Bayer processing [16]. Boehmite (aluminium monohydroxide or alumina monohydrate, $Al_2O_3.H_2O$ or γ-AlOOH) can be synthesized by hydrothermal processing at > 160 °C [17], or via crystallization from saturated sodium aluminate liquors by cooling [18,19]. Dash et al. reported that boehmite could be precipitated from a sodium aluminate solution having an A/C_{Na2O} of 1.0-1.1 at 85-93 °C (which is higher than the conditions for gibbsite precipitation) using > 300 g/L boehmite seeds. The addition of additives such as tartaric acid (50-300 mg/L) or precipitation at lower temperatures would favour the formation of gibbsite. A higher super-saturation also favours gibbsite formation [20]. Wang et al. used CO_2 to precipitate a mixture of gibbsite and boehmite from a sodium aluminate liquor as a method to recover aluminium hydroxide [21]. The use of flash calcination at 400-600 °C was applied to pre-treat a bauxite containing high aluminogoethite [22]. A thermal-chemical activation process was also developed by Smith and his co-workers to deal with high reactive silica bauxite [23,24]. The process involves the roasting of bauxites containing high reactive silica to ~950 °C or above to decompose the kaolin component into amorphous silica and transitional alumina. Roasting bauxite before its digestion can also potentially destroy most organic matter, which exist in the ore up to 0.5% w/w carbon [25]. While calcination of alumina at higher temperature is known its operational issues while processing is often not economical when processed in a tunnel kiln.

Moreover, the tunnel kilns are mostly used by the ceramic industries for heating refractory and ceramic products [26]. Basically, a tunnel kiln is a long stationary insulated furnace made of refractory bricks or pressed ceramic wool blankets. It has a rail track provision inside the kiln for the travel of trolleys. The material is loaded on the trolleys and enters from the feed end of the tunnel kiln [27]. It comes out on the other end by travelling inside the kiln with a prefixed speed. In these kilns, the material passes through different temperature regimes of preheating, and reduction as in beneficiated but with stationary bed of material [28]. Therefore, one has the flexibility with raw material. Another major advantage is that it utilizes beneficiated fines directly without induration. Low upkeep and maintenance are required. Unlike rotary kiln, heating is external and therefore it permits the use of different carbon source for heating. The only drawback of this process is low productivity which is even less compared to rotary kiln due to operational problems of charging powder alumina in the tunnel kiln using several containers or saggars which breaks due to thermal expansion during calcination at higher temperatures. This resulted frequent stoppages of kiln, new saggar replacements, loading and unloading issues etc. making business uneconomical.

2. Materials and Methods

Alumina was collected from the NALCO alumina refinery. PVA (Polyvinyl alcohol) was purchased from HIMEDIA. In the current research paper, we have tried to synthesize α-alumina by developing a suitable clot (pellets) by using of a suitable binder (which is a challenge) so that

alumina could be calcined without the use of saggar in tunnel kiln. The produced aluminium oxide is tested using various characterization techniques including XRD & SEM-EDS and the pellets physical properties with regard to is fragility under different parameters have been observed. Multiple experiments were performed for the synthesis of alumina with PVA. In addition, different weight quantities of PVA were tested for optimization procedures. Typically, 1 g, 2 g, 3 g and 4 g of PVA binder were included in the alumina-binder synthesis. For the experimental part, a consistent weight of alumina (25 g) was taken, and different amounts of PVA were added to it. The material was then, mixed, crushed well and stored in a dry container. Further, using a Hydraulic Press machine (PSi Analytics) different pellets were prepared. Each pellet was constructed with a uniform size at a pressure of 14 Pa (Pascal) unit. As can be seen in the images below, the pellets developed had an average diameter of 2.37 cm. These pellets are now ready for calcination process

3. Results and Discussion

3.1 Characterization

The investigation of the structure-property correlation of nanocomposites using X-ray diffraction spectroscopy technique is crucial. Since numerous fillers, nanoparticles, and other nanofibers have been utilised as reinforcement in nanocomposites, these investigations are crucial for analysing the characteristics. In determining the property variation and characterisation, factors such as, nanoparticle dispersion and its interaction with the matrix are crucial. Figure 1 shows the XRD analysis that was performed on the synthesised aluminium oxide and displays the XRD pattern corresponding to the α-Al_2O_3 phase. Figure 1 (a), (b), (c), (d), (e) and (f) represents XRD images of α-Al_2O_3 formation with different concentrations of PVA at 1000, 1100, 1200, 1300, 1400 and 1500 °C temperature respectively. The peak angles with their respective hkl planes have been described as: 25.5 ° (012), 35.0 ° (104), 37.7 ° (110), 43.5 ° (113), 52.5 ° (024), 57.5 ° (116), 66.4 ° (214) and 68.2 ° (300). However, it was observed that at lower temperatures, some phases of the generated aluminium oxide belong to the ɣ-phase. Thus, it is inferred that as the temperature is increased the crystallinity and alpha phase formation are favoured.

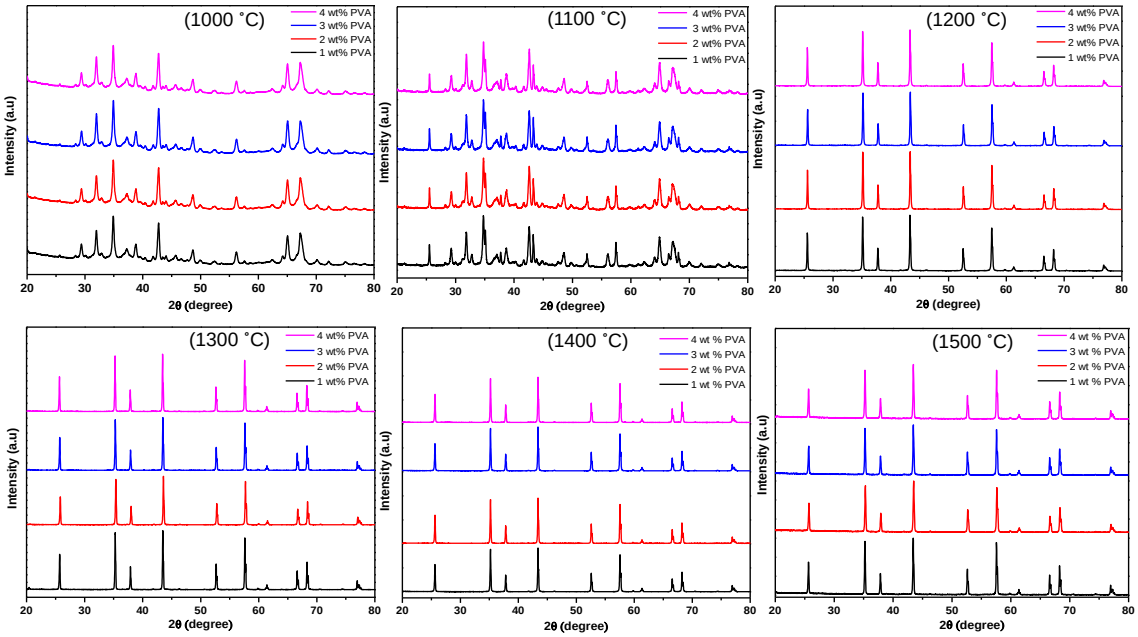

Figure 1. XRD pattern of α-alumina at (a) 1000 °C, (b) 1100 °C, (c) 1200 °C, (d) 1300 °C, (e) 1400 °C and (f) 1500 °C respectively.

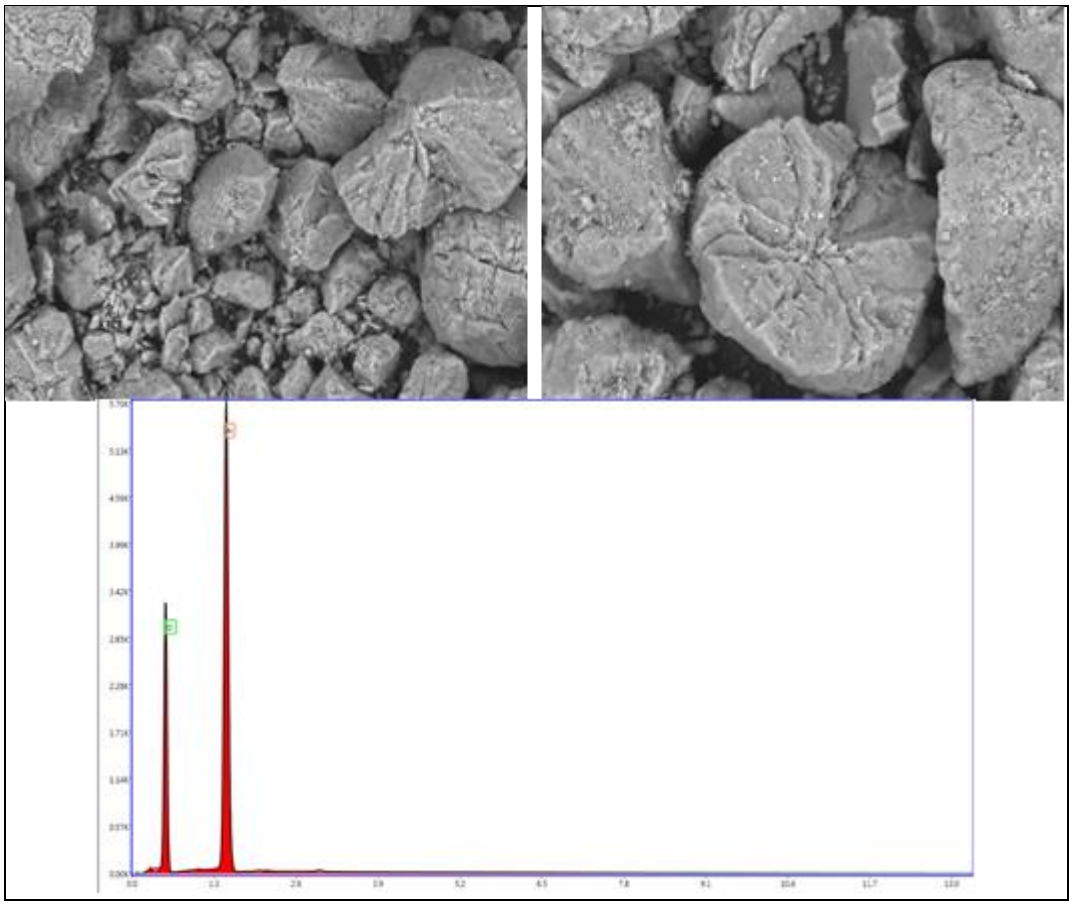

Figure 2. SEM-EDS image of the synthesized alpha aluminium oxide.

Understanding the particle distribution and its interactions with the matrix is also aided by SEM-EDS image and alpha phase formation by X-ray diffraction studies as evident from Figure 2. Scanning electron microscope (SEM) was used to examine the morphology and structure of the prepared samples. At different temperatures with various percentage of PVA, SEM-EDS were recorded and few are shown in Figure 2. It appeared to be very porous, with a large agglomeration size. EDS (Energy dispersive X-Ray spectroscopy) was used to determine the chemical compositions of the current aluminium oxide sample after annealing. The presence of aluminium and oxygen was confirmed by spectral analysis.

3.2 Effect of PVA as Binder

Before beginning the process, the most critical step is to choose a binder, because calcined alumina is a difficult material for binding and withstanding high temperature processing. The binders employed for synthesis of α-alumina is PVA (Polyvinyl alcohol). Here, we have selected PVA as the primary binder. This binder was considered as the most promising polymer due to its excellent water-soluble properties, good film forming capabilities, sound mechanical feature and most importantly, it is a good biodegradable chemical. Accordingly, detailed studies were undertaken using PVA.

3.3 Effect of Temperature

Calcination process involves the process of heating solids to a high temperature in order to remove volatile compounds. In the current investigation we evaluated different temperatures for each weight proportions of PVA in the pellet. For the calcination process, high temperatures ranging

from 1000 °C, 1100 °C, 1200 °C, 1300 °C, 1400 °C and 1500 °C for 2 hours with the residence temperature for 1 hour have been studied extensively. It was observed that all of the pellet constructions were found to be firmly held, ensuring that the experiment's goal was met. Furthermore, with temperature the colour change from off-white to bright white was very distinct, indicating that α-alumina was synthesized shown in Figure 3. Due to the vaporization of the volatile polymers, the particle size was clearly reduced to 2.24 cm. Each distinct weight measurements of synthesized pellet were calcined at the temperatures listed above and the results are shown below.

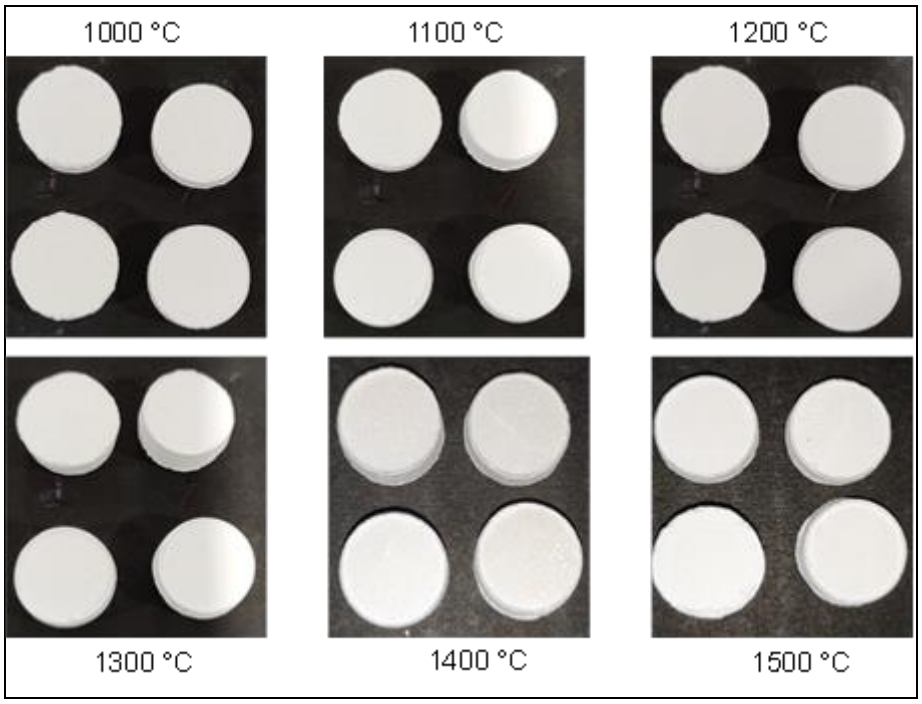

Figure 3. Alumina pellets after calcination process at different temperatures.

4. Conclusion

The experiments performed so far confirmed that the synthesized alumina is in its alpha phase. The pellet structure remained intact, with no major cracks, which could be an indication of evaporation of PVA during α-alumina production. Use of 1-2 percentage of PVA with alumina was found to be enough to provide binding efficiency to withstand disintegration of pellets during calcination at higher temperature. Only at 1500 °C, countable lines of cracks were observed (when 1-2% of PVA was used) without breakage of the Clots. There was no line of crack at lower temperatures. This aspect needs to be taken to a scaleup level under dynamic condition as the next step of work. While the clots were not strong (which is beneficial for further processing), they were not fragile also. Based on the XRD and SEM-EDS results, synthesis of calcined alumina alpha phase could be inferred with higher degree of alpha formation as the temperatures increases. Pellets prepared with a binder have a significant potential in industrial applications specially in handling alumina in kilns. The alumina powder when calcined in a kiln, especially in a tunnel kiln by putting them in several containers, the containers break during thermal expansion of alumina powders creating operational losses and handing problems. Alumina clot formation using a suitable binder is also not an easy process. The current paper exhibits the solution to such operational issue and could be taken forward to the next level of work.

5. References

1. C. Belver et al., Innovative W-doped titanium dioxide anchored on clay for removal of atrazine, *Catalysis Today*, Vol. 266, (2016), 36-45.
2. S. Klosek et al., Visible Light Driven V-Doped TiO_2 photocatalyst and its Photooxidation of ethanol, *The Journal of Physical Chemistry B*, Vol. 105, (2001), 2815 -2819.
3. G.K.Upadhyay et al., Synthesis of ZnO: TiO_2 nanocomposites for photocatalytic application in visible light, *Vacuum*, Vol. 160, (2019), 154 – 163.
4. A. Banishariff et al., Highly active Fe2O3-doped TiO2 photocatalyst for degradation of trichloroethylene in air under UV and visible light irradiation, *Applied Catalysis B*, Vol. 165, (2015), 209 – 221.
5. C. Karunakaran et al., Photocatalytic degradation of dyes by Al_2O_3-TiO_2 and ZrO_2-TiO_2 nanocomposites, *Materials Science Forum*, Vol. 734, (2013), 325-333.
6. D. Shchukin et al., TiO_2-In_2O_3 photocatalysts: preparation, characterizations and activity for 2-chlorophenol degradation in water, *Journal of Photochemistry and Photobiology* A: Chemistry, Vol. 162, (2004), 423-430.
7. N. Asong et al., The effect of iron doping on the adsorption of methanol on TiO_2 probed by sum frequency generation, *Chemical Physics*, Vol. 339, (2007), 86-93.
8. C. B. Maene et al., *International Journal of Applied Engineering Research*, Vol. 13,19 (2018),14372–14377.
9. S. Ameene et al., Solution-processed CeO_2/TiO_2 nanocomposite as potent visible light photocatalyst for the degradation of bromophenol dye, *Chemical Engineering Journal*, Vol. 247, (2014), 193-198.
10. X. Gao et al., Preparation and characterization of CeO_2/TiO_2 catalysts for selective catalytic reduction of NO with NH_3, *Catalysis Communications*, Vol. 11.5, (2010), 465-469.
11. U. Qureshi et al., Nanoparticulate cerium dioxide and cerium dioxide–titanium dioxide composite thin films on glass by aerosol assisted chemical vapor deposition, *Applied Surface Science*, Vol. 256.3, (2009), 852-856.
12. F. Galindo et al., Photodegradation of the herbicide 2, 4-dichlorophenoxyacetic acid on nanocrystalline TiO_2–CeO_2 sol–gel catalysts, *Journal of Molecular Catalysis A: Chemical*, Vol. 281, (2008), 119-125.
13. K. Evans et al., The History, Challenges, and New Developments in the Management and Use of Bauxite Residue, *Journal of Sustainable Metallurgy*, Vol. 2, (2016), 316–331.
14. W. M. Mayes et al., Advances in Understanding Environmental Risks of Red Mud After the Ajka Spill, Hungary, *Journal of Sustainable Metallurgy*, Vol. 2, (2016), 332–343.
15. J.B. Goloran et al., Selecting a nitrogen availability index for understanding plant nutrient dynamics in rehabilitated bauxite-processing residue sand, *Ecological Engineering*, Vol. 58, (2013), 228-237.
16. Union, Innovation. "Communication from the Commission to the European Parliament, the Council, the European Economic and Social Committee and the Committee of the Regions", *A new skills agenda for Europe*, Brussels (2014).
17. A.K. Yadav et al., Toxic characterization of textile dyes and effluents in relation to human health hazards, *Journal of Sustainable Environment Research*, Vol. 3.1, (2014), 95-102.
18. P. Ji et al., Study of adsorption and degradation of acid orange 7 on the surface of CeO_2 under visible light irradiation, *Applied Catalysis B: Environmental*, Vol. 85, (2009),148-154.
19. M. Zhu et al., Synthesis of porous Fe_3O_4 nanospheres and its application for the catalytic degradation of xylenol orange, *The Journal of Physical Chemistry C*, Vol. 115.39, (2011), 18923-18934.
20. A.V.P. Rao et al., Non-TiO_2 Based Photocatalysts for Remediation of Hazardous Organic Pollutants under Green Technology-Present Status: A Review." *Journal Applicable Chemistry*, Vol. 4.4, (2015), 1145-72.
21. V. Iliev., et al., Photooxidation of xylenol orange in the presence of palladium-modified TiO_2 catalysts, *Catalysis Communications*, Vol. 5.12, (2004), 759-763.

22. J. Tian et al., Enhanced photocatalytic performances of CeO_2/TiO_2 nanobelt heterostructures, *Small*, Vol. 9.22, (2013), 3864-3872.
23. K. Kasinathan et al., Photodegradation of organic pollutants RhB dye using UV simulated sunlight on ceria based TiO_2 nanomaterials for antibacterial applications, *Scientific reports*, Vol. 6.1, (2016), 1-12.
24. M. Li et al., A thermally stable mesoporous ZrO_2–CeO_2–TiO_2 visible light photocatalyst, *Chemical Engineering Journal*, Vol. 229, (2013), 118-125.
25. D. Lee et al., The TiO_2-adding effects in WO_3-based NO_2 sensors prepared by coprecipitation and precipitation method, *Sensors and Actuators B: Chemical*, Vol. 65, (2000), 331-335.
26. Z. Jiang et al., Catalytic properties of silver nanoparticles supported on silica spheres, *The Journal of Physical Chemistry B*, Vol. 109.5, (2005), 1730-1735.
27. F. U. Khan et al., Antioxidant and catalytic applications of silver nanoparticles using Dimocarpus longan seed extract as a reducing and stabilizing agent, *Journal of Photochemistry and Photobiology B: Biology*, Vol. 164, (2016), 344-351.
28. C. W. Gray et al., Field evaluation of in situ remediation of a heavy metal contaminated soil using lime and red-mud, *Environmental Pollution*, Vol. 142.3, (2006), 530-539.